INSTITUTE OF PHYSICS PUBLISHING JOURNAL OF MICROMECHANICS AND MICROENGINEERING

J. Micromech. Microeng. **16** (2006) 1579–1586 doi:10.1088/0960-1317/16/8/019

A miniature 1×2 mechanical optical switch with anti-thermal design

Tien-Tung Chung, Chen-Cheng Lee, Kuang-Chao Fan, Wu-Lang Lin, Jian-Gou Peng and Hsu Fan

Department of Mechanical Engineering, National Taiwan University, Taipei 10617, Taiwan, Republic of China

E-mail: ttchung@ntu.edu.tw

Received 9 February 2006, in final form 19 May 2006
Published 29 June 2006
Online at stacks.iop.org/JMM/16/1579

Abstract

This paper describes the study on an innovative miniature 1×2 mechanical optical switch with anti-thermal design. Firstly, a novel switch configuration with line-to-line and fiber-to-fiber alignments is designed. An included anti-thermal mechanism is proposed by utilizing materials with different thermal expansion coefficients to compensate the axial misalignment due to ambient temperature changes. Then, parametric programs to automatically generate the solid model and to analyze thermal behavior of the switch are developed. Finally, a prototype is fabricated and the temperature cycling tests of Bellcore specifications are carried out. According to experimental measurements, it is found that the insertion loss of the prototype satisfies the requirements of Bellcore specifications. This 1×2 mechanical optical switch is small, thermally balanced and reliable.

(Some figures in this article are in colour only in the electronic version)

1. Introduction

In an era of rising popularity of the Internet, fiber-optic networking is becoming more and more important in high-speed data transmission because of its characteristics of low-loss, lightweight and high-bandwidth. The optical switch is essential in an optical communication system because it maps wavelength from input ports to appropriate output ports based on their destination. In recent years, research on the design of optical switches has grown rapidly. The optic-electro-optic (O-E-O) optical switch is presented in [1, 2]. In O-E-O optical switches, optical signals from the input fiber will be converted into electronic signals first, which then pass through an electronic converter switch to the required output channel. Passing through an electro-optic (E-O) converter, the output optical signals can then couple to the output fiber. However, devices using O-E-O contain several drawbacks, such as the requirement of expensive optic-electro (O-E) conversion devices, high cross talk and the electronic limit in the growth of bandwidth. The all-optic (optic-optic-optic, O-O-O) switching design is potentially capable of eliminating these disadvantages [3, 4]. Nevertheless, as compared to the O-O-O type of optical switches, the mechanical type still dominates the market because of its low cost. Chang *et al* [5] developed a mechanical switching apparatus comprised of an output fiber alignment head with a V-groove and a switching member arranged to pivot between first and second positions. The design of this switching mechanism leads to bending of the input fiber tip when the fiber is pushed against the V-groove. This kind of optical switch still encounters difficulties in meeting the requirements of increasing capacity and Bellcore specifications because of the need to adapt to various environments. It is especially true when a change of ambient temperature results in axial misalignments of the input and output fiber tips due to different thermal expansion coefficients of switch component materials. In response to this kind of thermal misalignment problem, a proper anti-thermal mechanism is necessary. Morey and Glomb [6] developed a temperature-compensated optical waveguide light filtering device. The fiber is attached to two compensating members made of materials with different thermal expansion coefficients. In this device, the lengths of both the compensating members and the optical fibers will be changed to compensate the misalignment. Yoffe *et al* [7] assembled a passive temperature-compensating package for fiber gratings. The grating is mounted in a package consisting

Table 1. Bellcore specifications for the optical switch.

Temperature cycling tests	From −5 °C to 75 °C
Insertion loss requirement	Less than 1 dB

of two materials with different thermal expansion coefficients. A silica tube is used as the low thermal expansion component and an aluminum tube works as the high thermal expansion component. In this design, the aluminum tube is used as the compensating member during ambient temperature changes. While different temperature compensating designs are used in filtering devices and fiber gratings, systematic methods for applying anti-thermal designs in optical switches are however lacking. This is the goal of this study. Previous work by the authors has developed a miniature and low-cost 1×2 optical switch [8]. This study is the extended work of the switch to include the thermal compensation design.

2. Design of a 1×2 optical switch with an anti-thermal mechanism

The goal of this study is to design a new miniature 1×2 mechanical optical switch with an anti-thermal mechanism to balance the axial misalignment of fibers due to ambient temperature changes. Design requirements of this new switch should meet the following conditions: small size, low optical loss, low thermal effects and reliable performance.

2.1. The design concept

As shown in table 1, the design specifications of the switch take the temperature cycling tests and insertion loss requirements into account. In the standard temperature cycling tests, the switch should be subjected to an ambient temperature change from −5 °C to 75 °C. In the standard insertion loss requirements, an insertion loss of less than 1 dB should be maintained in the multi-mode fiber with a core diameter of 62.5 μm. Dautartas *et al* [9] and Sutherland *et al* [10] performed the experiments to build the relations between fiber tips misalignments and the insertion loss, and their results are adopted as our design requirements. Therefore, the axial and transverse misalignments are controlled to within 25 μm and 10 μm, respectively, in this paper.

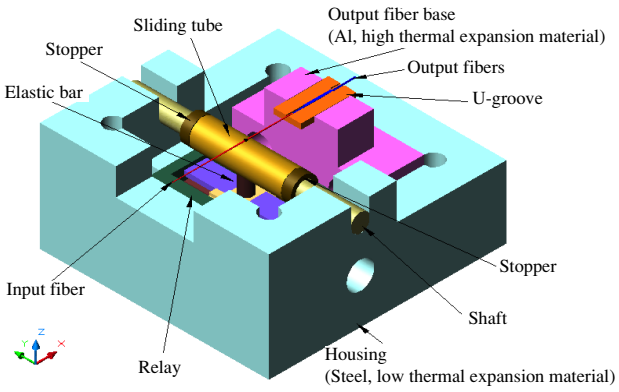

Figure 2. The configuration of the 1×2 mechanical optical switch.

As shown in figure 1, a novel switching mechanism for the 1 × 2 mechanical optical switch is designed based on the line-to-line and fiber-to-fiber principles. This design eliminates some conventional parts, such as the collimators, turning mirrors [11] and prisms [12] for structural simplicity. It also has low power consumption. In this design, the input fiber is mounted onto a sliding tube and the two output fibers are mounted onto a U-groove fiber holder with a dimension of 12 × 3 × 0.5 mm^3. The U-groove is 125 μm in depth and 250 μm in width. The sliding tube and two tube stoppers are assembled in a shaft. A mechanical relay is used to switch the sliding tube to one of the two tube stoppers such that the input fiber can be aligned precisely to one of the two output fibers. The configuration of this 1×2 mechanical optical switch is shown in figure 2.

2.2. Anti-thermal mechanism design

As shown in figure 3, an anti-thermal mechanism with a high thermal expansion base and a low thermal expansion housing is proposed. When the ambient temperature is changed, non-uniform thermal expansion of internal components will result in the misalignment of the input and output fiber tips. The sizes of these two bases can be particularly designed to compensate for this misalignment. The stainless steel alloy, with a thermal expansion coefficient of 12.4 × 10^{-6} °C^{-1}, can be chosen as the low thermal expansion housing material, and aluminum alloy,

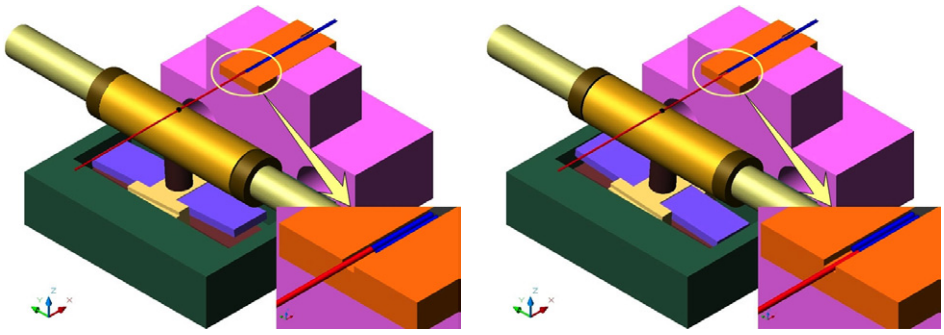

(*a*) (*b*)

Figure 1. Two switching positions of the novel switching mechanism: (*a*) right position and (*b*) left position.

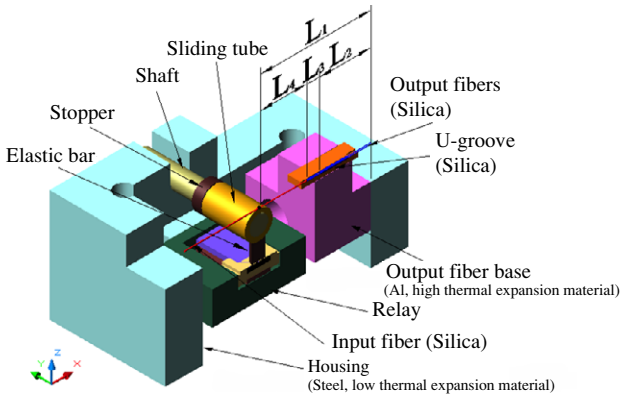

Figure 3. Cross-sectional view of the 1×2 optical switch.

with a thermal expansion coefficient of $24 \times 10^{-6}\,^{\circ}\mathrm{C}^{-1}$, can be chosen as the high thermal expansion base material. As shown in figure 3, the dimensions of the anti-thermal mechanism can be decided using the following equations:

$$\alpha_{\mathrm{St}} L_1 \Delta T = [\alpha_{\mathrm{Al}} L_2 + \alpha_{\mathrm{Si}}(L_3 + L_4)]\Delta T, \tag{1}$$

$$L_1 = L_2 + L_3 + L_4, \tag{2}$$

where $\vec{L} = (L_1, L_2, L_3, L_4)$ are the component sizes of the anti-thermal mechanism, ΔT is the ambient temperature change, α_{St} is the thermal expansion coefficient of stainless steel alloy (low thermal expansion coefficient material), α_{Al} is the thermal expansion coefficient of aluminum alloy (high thermal expansion coefficient material) and α_{Si} is the thermal expansion coefficient of the silica (material for U-groove fiber holder, input and output fibers).

Based on the thermal balance of equations (1) and (2), a set of component sizes can be decided for the anti-thermal mechanism design. One set of sizes $\vec{L}$ = (12.0 mm, 6.0 mm, 1.4 mm, 4.6 mm), which satisfies equations (1) and (2), is selected for the anti-thermal design. In order to investigate the response variations with respect to these four parameters, the axial misalignment $d_{\mathrm{a}}(\vec{L})$ between fiber tips due to change of the ambient temperature can be defined as the difference between the left-hand side and the right-hand side of equation (1). It can be expressed as

$$d_{\mathrm{a}}(\vec{L}) = [\alpha_{\mathrm{St}} L_1 - \alpha_{\mathrm{Al}} L_2 - \alpha_{\mathrm{Si}}(L_3 + L_4)]\Delta T. \tag{3}$$

For any set of sizes that satisfies equations (1) and (2), the axial misalignment is equal to zero, i.e. $d_{\mathrm{a}}(\vec{L}) = 0$. In addition, the sensitivities of the axial misalignment $d_{\mathrm{a}}(\vec{L})$ with respect to these component sizes can be analyzed by differentiating $d_{\mathrm{a}}(\vec{L})$ with respect to L_1, L_2, L_3 and L_4, respectively as follows:

$$\frac{\partial d_{\mathrm{a}}(\vec{L})}{\partial L_1} = \alpha_{\mathrm{St}}\Delta T = 12.4 \times 10^{-6}\Delta T, \tag{4}$$

$$\frac{\partial d_{\mathrm{a}}(\vec{L})}{\partial L_2} = -\alpha_{\mathrm{Al}}\Delta T = -24 \times 10^{-6}\Delta T, \tag{5}$$

$$\frac{\partial d_{\mathrm{a}}(\vec{L})}{\partial L_3} = \frac{\partial d_{\mathrm{a}}(\vec{L})}{\partial L_4} = -\alpha_{\mathrm{Si}}\Delta T = -0.8 \times 10^{-6}\Delta T. \tag{6}$$

From equations (4)–(6), derivatives of $d_{\mathrm{a}}(\vec{L})$ with respect to L_1 and L_2 are more sensitive to those with respect to L_3 and L_4. Hence, when redesign is required, it is more effective to change sizes of L_1 and L_2 than to change sizes of L_3 and L_4.

There are several advantages of this novel optical switch design:

(1) The line-to-line and fiber-to-fiber configurations promise less insertion loss than other mechanical optical switches with light bending configurations [5].
(2) An anti-thermal mechanism is designed to compensate for the axial misalignment between the input fiber and the output fiber tips when ambient temperature changes.
(3) Simpler configuration yields an easier and precise assembly process.
(4) Compared to traditional optical switches, it omits the collimators and prisms so as to reduce the device size ($25 \times 26 \times 12$ mm^3) and cost.

The optical switch design presented in this paper has to pass the temperature cycling tests in accordance with Bellcore specifications. Therefore, thermal responses of the anti-thermal mechanism and optical switch are analyzed using the commercial finite element analysis software ANSYS. It is assumed that all components of the optical switch are manufactured and assembled at 25 °C.

2.3. Thermal responses of the switch with and without the anti-thermal design

In order to show the improvements of the switch with anti-thermal design (using different thermal expansion materials) against the switch without anti-thermal design (using the same thermal expansion material), thermal responses of the two switches will be analyzed and results will be compared. The switch with anti-thermal design is shown in figure 3, and the component sizes are $\vec{L}$ = (12.0 mm, 6.0 mm, 1.4 mm, 4.6 mm). For the switch without anti-thermal design, the configuration and component sizes are the same; however, the same thermal expansion material (steel) is used in both the housing and the output fiber base.

The solid model of the switch is originally generated in AutoCAD from given component sizes. The solid model is exported to an ACIS SAT file by AutoCAD, and then imported to ANSYS to establish the finite element meshes. The solid element type SOLID45 is used to simulate the thermal and structural responses of the switch. In the analysis model, two cases of thermal boundary conditions are applied:

- Case 1: the temperature of all components changes uniformly from 25 °C to 75 °C
- Case 2: the temperature of all components changes uniformly from 25 °C to −5 °C.

After applying these boundary conditions to the finite element model, thermal responses of the switches with and without the anti-thermal design can be computed by ANSYS. The results are compared as shown in figures 4 and 5. Figure 4(*a*) shows results without the anti-thermal design when temperature changes from 25 °C to 75 °C (case 1). In figure 4(*a*), the low thermal expansion material (steel) used in housing and the output fiber base separates the input

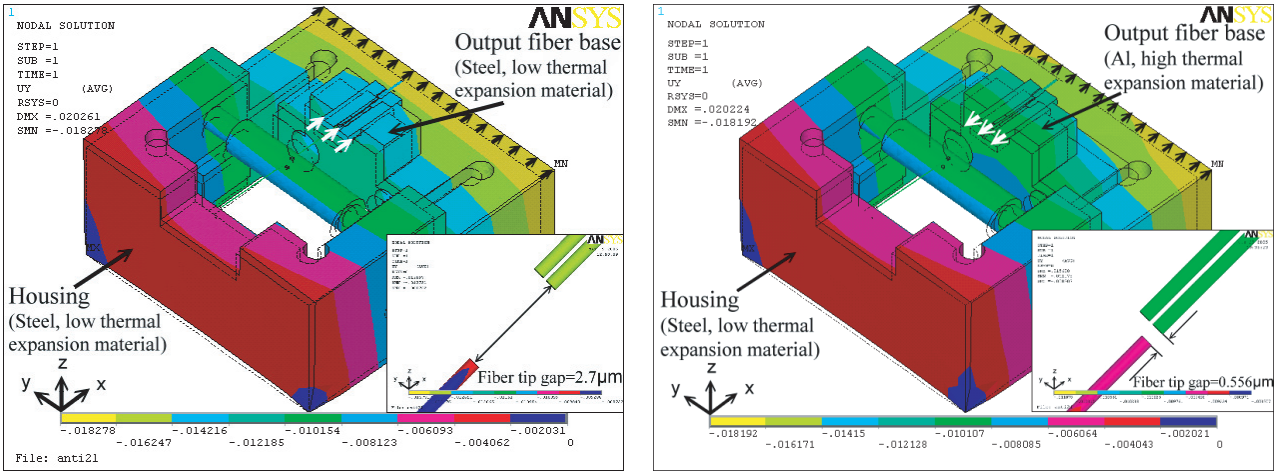

(*a*) (*b*)

Figure 4. Thermal deformation (mm) in the axial direction of case 1 (temperature changes from 25 °C to 75°): (*a*) switch without anti-thermal design and (*b*) switch with anti-thermal design.

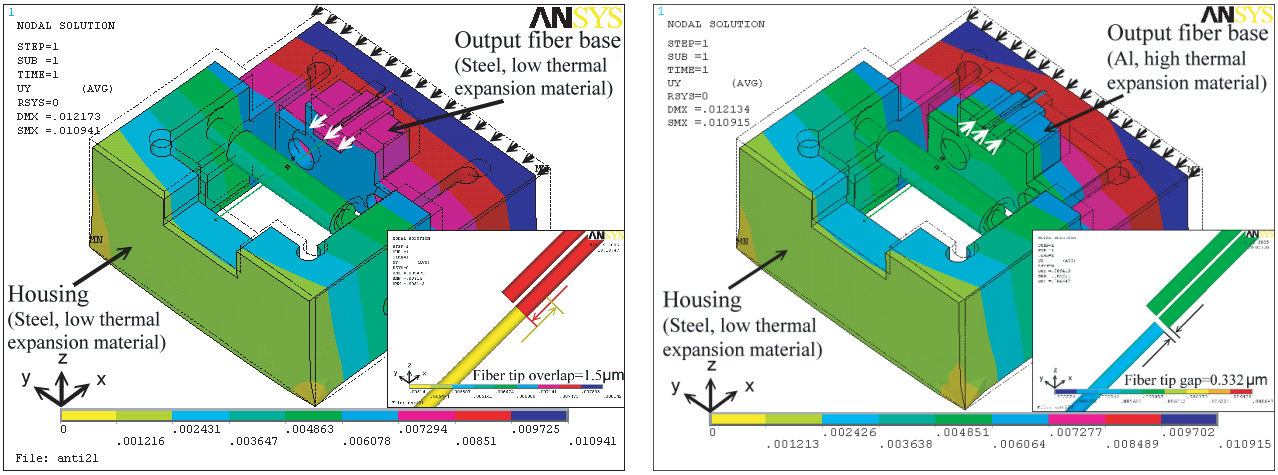

(*a*) (*b*)

Figure 5. Thermal deformation (mm) in the axial direction of case 2 (temperature changes from 25 °C to −5°): (*a*) switch without anti-thermal design and (*b*) switch with anti-thermal design.

and output fiber tips apart in the axial direction and causes the axial misalignment. Figure 4(*b*) shows results with the anti-thermal design when temperature changes from 25 °C to 75 °C (case 1). In figure 4(*b*), the housing (with low thermal expansion material) separates the input and output fiber tips apart in the axial direction, and the output fiber base (with high thermal expansion material) compensates this axial misalignment. In addition, the axial misalignment is 0.556 μm with anti-thermal design compared to the value of 2.7 μm without anti-thermal design. It has 79% ((2.7 μm − 0.556 μm)/2.7 μm) improvement on axial misalignment between two fiber tips for case 1.

Figure 5(*a*) shows results without the anti-thermal design when temperature changes from 25 °C to −5 °C (case 2). In figure 5(*a*), the same low thermal expansion material (steel) used in housing and the output fiber base brings the input and output fiber tips closer in the axial direction and causes the overlap of fiber tips, which could damage the fiber tips. Figure 5(*b*) shows results with the anti-thermal design when temperature changes from 25 °C to −5 °C (case 2). In figure 5(*b*), the housing (with low thermal expansion material) brings the input and output fiber tips closer in the axial direction and the output fiber base (with high thermal expansion material) compensates this axial misalignment. In addition, the axial misalignment is 0.332 μm with anti-thermal design compared to the value of 1.5 μm without anti-thermal design. It has 78% ((1.5 μm − 0.332 μm)/1.5 μm) improvement on axial misalignment between two fiber tips for case 2.

The thermal deformation result of the switch with anti-thermal design is shown in table 2. In case 1, the thermal deformations of the input and output fiber tips in the axial direction are 9.400 μm and 9.956 μm respectively; therefore the axial departure of fiber tips is 0.566 μm, as shown in figure 4(*b*). In case 2, the thermal deformations of the input and output fiber tips in the axial direction are −5.540 μm and −5.872 μm respectively; therefore the axial gap of fiber tips is −0.332 μm, as shown in figure 5(*b*). The analyzed axial misalignments of fiber tips in these two cases are

Table 2. Thermal deformation of the switch with anti-thermal design in the axial direction.

	Input fiber tip deformation (μm)	Output fiber tip deformation (μm)	Axial misalignment (μm)
Case 1: temperature changes from 25 °C to 75 °C	9.400	9.956	0.556
Case 2: temperature changes from 25 °C to −5 °C	−5.540	−5.872	−0.332

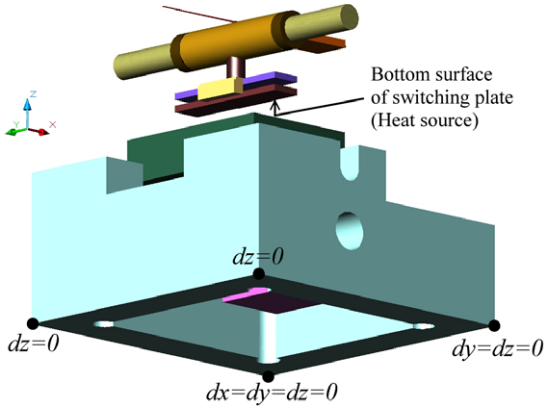

Figure 6. Thermal loading and structural boundary conditions of the optical switch.

Table 3. Properties of the actuator.

Voltage amplitude (V)	5	
Coil resistance (Ω)	125	
Area of heat source (mm^2)	31.22	
Heat generation rate of the electric wire per unit area (W mm^{-2})	3.2×10^{-3}	
Hydraulic diameter (mm)	22.4	
Thermal conductivity of air (W (mm °C)$^{-1}$)	$T = 75$ °C	2.96×10^{-5}
	$T = 25$ °C	2.55×10^{-5}
	$T = -5$ °C	2.37×10^{-5}
Convective heat transfer coefficient of air flow (W (mm^2 °C)$^{-1}$)	$T = 75$ °C	4.78×10^{-6}
	$T = 25$ °C	4.11×10^{-6}
	$T = -5$ °C	3.82×10^{-6}

much smaller than the requirement of 25 μm as indicated in section 2.1. Therefore, the analysis results demonstrate that the anti-thermal mechanism can reduce axial misalignment of fiber tips.

2.4. Internal heat generation of the optical switch

The thermal behaviors are explained in terms of mass, thermal properties, internal heat generation, conduction heat flow and convection heat flow of the structure. Radiation heat flow of the switch is negligible and is thus disregarded in the thermal analysis.

The electric wire in the actuator serves as the main heat source of the switch [13]. As shown in figure 6, the bottom surface of the switching plate, to which the electric wire is adhered, is assumed to be the only heat source in the thermal analysis. Furthermore, the heat generation is presumed to be uniformly distributed over this surface. The heat generation rate of the electric wire per unit area $\dot{Q}$ can be evaluated by the following equations [14]:

$$V(t) = V_n \sin(\omega t), \tag{7}$$

$$Q(t) = I(t)V(t) = \frac{V^2(t)}{R} = \frac{V_n^2 \sin^2(\omega t)}{R}, \tag{8}$$

$$\dot{Q} = \frac{\left(\int_0^{\pi/\omega} Q(t)\,\mathrm{d}t\right)\Big/\left(\frac{\pi}{\omega}\right)}{A} = \frac{\frac{\omega}{\pi}\int_0^{\pi/\omega} V_n^2 \sin^2(\omega t)\,\mathrm{d}t}{RA} = \frac{V_n^2}{2RA}, \tag{9}$$

where $V(t)$ is the voltage at time t, V_n is the voltage amplitude, ω is the frequency, $Q(t)$ is the heat generation of the electric wire at time t, $I(t)$ is the current at time t, R is the coil resistance and A is the area of heat source.

Estimating the convective heat transfer coefficients of the air flowing in the switch is a prerequisite for thermal analysis of the switch. The air flowing in the square cross-sectional switch is assumed to be laminar, thermally fully developed and with uniform heat flux. In this situation, the Nusselt number Nu for heat transfer is generally described as $Nu = 3.614$ [15]. Therefore, the convective heat transfer coefficient of the air in the switch h can be estimated by the following equation:

$$h = \frac{Nu \cdot k}{D_\mathrm{h}}, \tag{10}$$

where h is the convective heat transfer coefficient of air flow, k is the thermal conductivity of air and D_h is the hydraulic diameter. For the current design, D_h is calculated as [16]

$$D_\mathrm{h} = \frac{4A_\mathrm{c}}{P} = \frac{4 \cdot (22 \cdot 23)}{2 \cdot (22 + 23)} = 22.4\ (\mathrm{mm}), \tag{11}$$

where A_c is the cross-section area (mm^2) and P is the perimeter (mm).

The heat transfer coefficients of the air in the switch for temperatures at −5 °C, 25 °C and 75 °C are computed according to equation (10) and shown in table 3. The electrical and thermal properties of the actuator are also recorded in table 3.

2.5. Thermal analysis of the optical switch

The solid model of the optical switch is originally generated in AutoCAD from given design parameters. The model is exported to an ACIS SAT file by AutoCAD, and then imported to ANSYS to establish the finite element meshes for the switch as shown in figure 7. The material properties of the switch components are listed in table 4. The number of nodal points and the degrees of freedom needed for the switch depend on the complexity of the design and the required level of precision of the analysis. In ANSYS, solid element type SOLID70 is used for simulating the temperature distribution analysis and SOLID45 for thermal responses. In the analysis model, three

Table 4. Material properties of the switch components.

Material	Switch components	Young's modulus (kgf mm^{-2})	Poisson ratio	Thermal conductivity (W (mm °C)$^{-1}$)	Thermal expansion coefficient (°C^{-1})
Silica	Multi-mode fiber, U-groove	7749	0.17	1.4×10^{-3}	0.8×10^{-6}
Al alloy	High thermal expansion base	7300	0.3	10×10^{-3}	24×10^{-6}
Steel alloy	Low thermal expansion housing	21 122	0.3	51.9×10^{-3}	12.4×10^{-6}

Table 5. Thermal analysis results of the optical switch.

Misalignments	Case 1: ambient temperature changes from 25 °C to 75 °C	Case 2: ambient temperature changes from 25 °C to −5 °C	Case 3: ambient temperature is 25 °C
Axial misalignment (μm)	0.792	0.426	0.003 12
Transverse misalignment (μm)	0.0813	0.0623	0.002 84

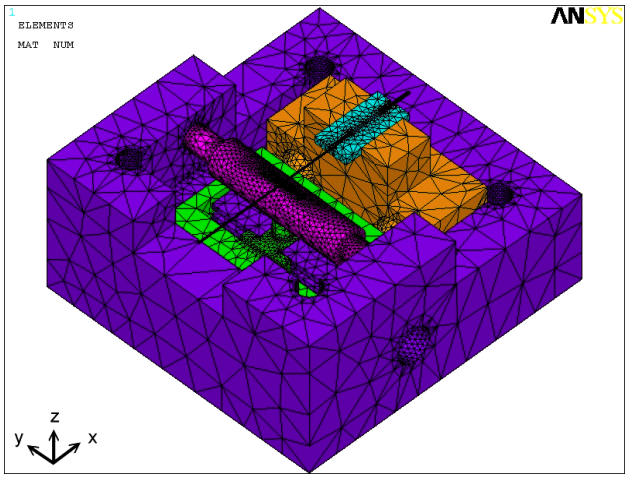

Figure 7. Meshed model of the optical switch.

cases of thermal boundary conditions are applied:

- Case 1: the ambient temperature changes from 25 °C to 75 °C
- Case 2: the ambient temperature changes from 25 °C to −5 °C
- Case 3: the ambient temperature is 25 °C.

After applying these boundary conditions and heat generation thermal loadings to the finite element model, the steady-state temperature distributions can be computed by ANSYS. After obtaining the non-uniform temperature distributions of the switch structure, ANSYS can determine the thermal deformation of the switch with structural boundary conditions set forth in figure 6.

The thermal deformations of the optical switch under the boundary conditions of case 1, case 2 and case 3 are shown in figures 8(*a*)–(*c*), respectively. As shown in figure 8(*a*) the fiber tips bend up, in figure 8(*b*) the fiber tips bend down and in figure 8(*c*) the fiber tips bend up slightly. These phenomena can be explained briefly as follows. As shown in figure 3, the U-groove is made up of silica with a thermal expansion coefficient of 0.8×10^{-6} °C^{-1}, and the output fiber base is made up of aluminum with 24.0×10^{-6} °C^{-1}. The bottom face of the U-groove is glued onto the top face of the output fiber base. It is also noted that the switch is assembled at the ambient temperature 25 °C. Under the boundary conditions of case 1 and case 3, the temperature of the U-groove and output fiber base is higher than 25 °C, and the bottom face of the U-groove is stretched by the aluminum base which has a larger thermal expansion coefficient. Hence, the U-groove will be bended up, and the output fibers mounted on the top of the U-groove will also be bended up. Under the boundary condition of case 2, the temperature of the U-groove and output fiber base is lower than 25 °C, the bottom face of the U-groove will be shrunk by the aluminum base, and both the U-groove and output fibers will be bended down. As for the input fiber, when the housing temperature is higher than 25 °C, it will be moved up vertically. When the housing temperature is lower than 25 °C, the input fiber will be moved down vertically.

The thermal analysis results are recorded in table 5. The axial and transverse misalignments of fiber tips are 0.792 μm and 0.0813 μm in case 1, 0.426 μm and 0.0623 μm in case 2 and 0.003 12 μm and 0.002 84 μm in case 3. The analysis results indicate that the axial and transverse misalignments in all three cases are less than 25 μm and 10 μm respectively, and thus satisfy the design requirements of the optical switch.

3. Temperature cycling tests

As shown in the previous analysis results, the proposed optical switch design satisfies design requirements when the ambient temperature changes between −5 °C and 75 °C. A prototype of this design is fabricated. During the assembly process of the optical switch, a computer-assisted automatic alignment system is used for precision alignment between input and output fibers [17]. Figure 9 shows a photo of the prototype of the developed 1 × 2 optical switch.

After the packaging and alignment processes, the temperature cycling tests of Bellcore specifications are carried out. The optical fibers used in this study are of the following specifications: multi-mode fiber, outer diameter 125 μm, core diameter 62.5 μm, zero degree of the tip and without any anti-reflective coating. As shown in figure 10, the complete optical switch system is placed in a mini environment chamber in which the temperature and humidity can be controlled by computer.

In the standard temperature cycling tests, the insertion loss has to be kept within 1 dB when the ambient temperature changes from −5 °C to 75 °C. In the temperature cycling

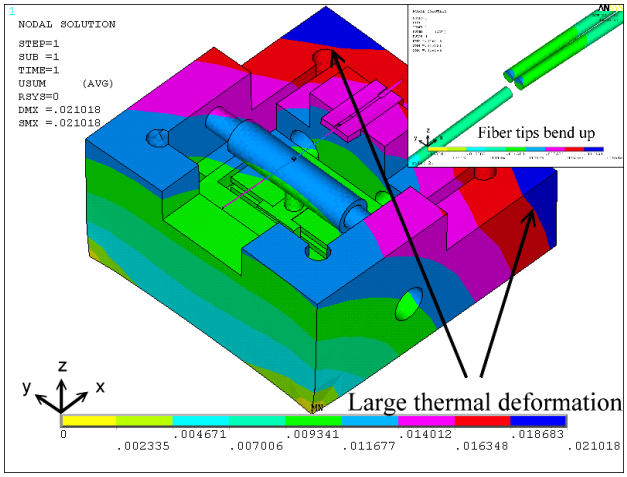

(*a*)

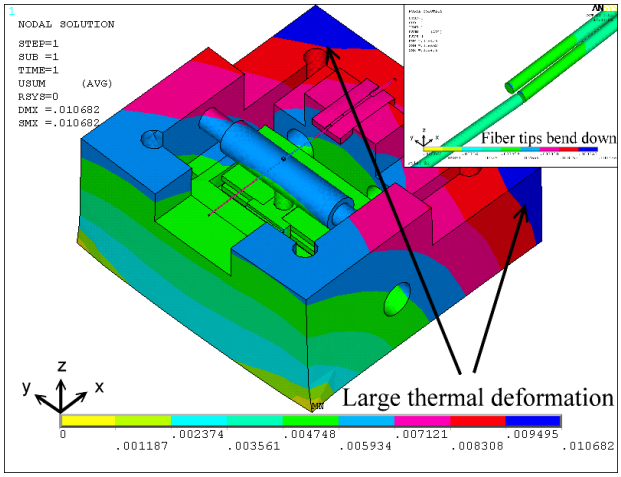

(*b*)

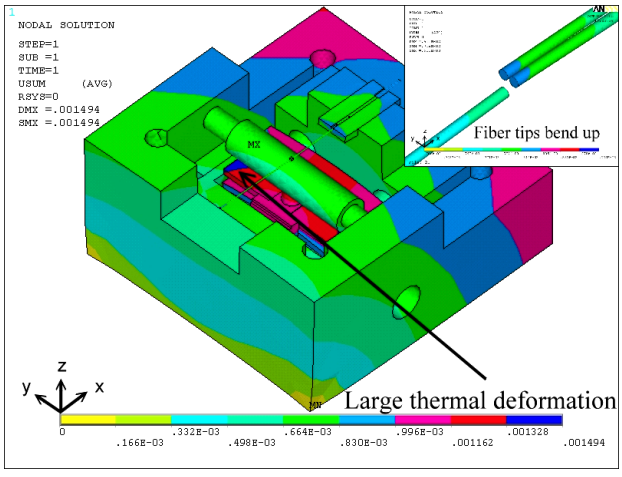

(*c*)

Figure 8. Thermal deformation (mm) of the optical switch. (*a*) Thermal deformation (mm) distribution in case 1: temperature changes from 25 °C to 75 °C. (*b*) Thermal deformation (mm) distribution in case 2: temperature changes from 25 °C to −5 °C. (*c*) Thermal deformation (mm) distribution in case 3: temperature is 25 °C.

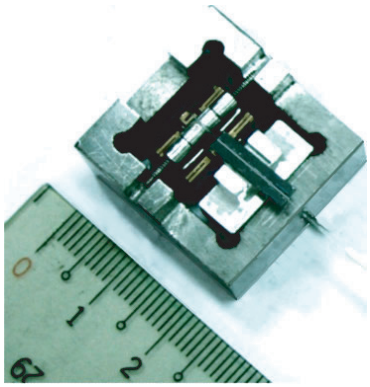

Figure 9. Photo of the developed 1 × 2 optical switch.

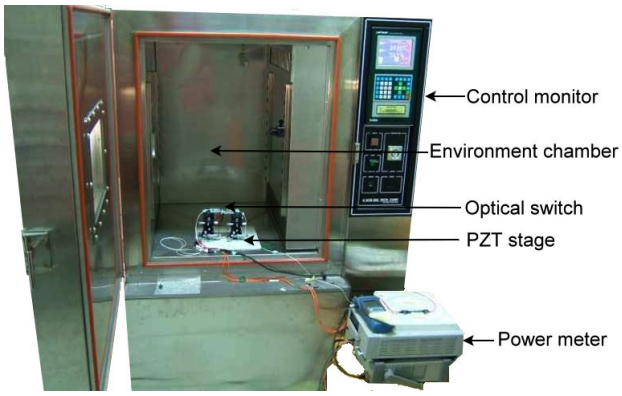

Figure 10. Photo of the mini environment chamber with the optical switch inside.

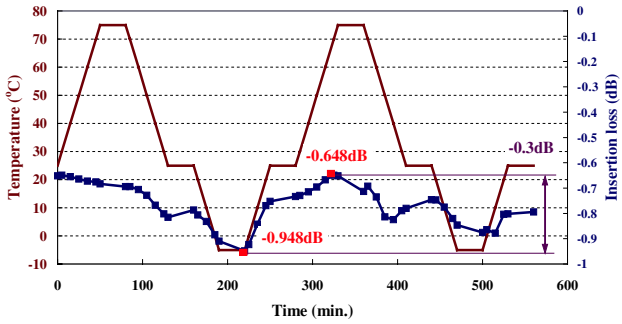

Figure 11. Result of temperature cycling tests.

tests, the ambient temperature rises from 25 °C to 75 °C and remains constant at 75 °C for 30 min, then drops back to 25 °C and remains at 25 °C for 30 min, then continuously drops to −5 °C and remains at −5 °C for 30 min. Finally the ambient temperature rises back to 25 °C and remains at 25 °C for 30 min. The whole procedure mentioned above is repeated twice. As shown in figure 11, the insertion loss varies slightly when the temperature rises and drops. The maximum and minimum insertion losses are 0.948 dB and 0.648 dB respectively, which are less than 1 dB during the entire temperature cycling tests and thus satisfy the Bellcore specifications. In addition, the insertion loss variation is

only 0.3 dB, which is very small. Therefore, the temperature cycling tests demonstrate that the anti-thermal mechanism can reduce the misalignment of fiber tips to only very small amount of insertion loss variation.

4. Conclusions

This paper describes the study on an innovative miniature 1×2 mechanical optical switch with anti-thermal design. A novel and simple optical switch design, with a small dimension of only $25 \times 26 \times 12$ mm^3, line-to-line and fiber-to-fiber configuration is designed. An anti-thermal mechanism is included to compensate the axial misalignment of fiber tips due to ambient temperature changes. The thermal responses of the optical switch are computed by ANSYS. The analysis results demonstrate that the axial and transverse misalignments of the fiber tips are less than 25 μm and 10 μm respectively. Then, a prototype is fabricated and the temperature cycling tests of Bellcore specifications are carried out. The experiment's results show that the insertion loss of fiber tips can be controlled within 0.948 dB with only 0.3 dB insertion loss variation during the temperature cycling tests. The experimental results of the developed optical switch conform to the Bellcore specifications. This miniature 1×2 mechanical optical switch is small, of low thermal effects and reliable.

References

[1] Olbright G R, Bryan R P, Lear K, Brennan T M, Poirier G, Lee Y H and Jewell J L 1991 Cascadable laser logic devices: discrete integration of phototransistors with surface-emitting laser diodes *Electron. Lett.* **27** 216–7

[2] Bourouha M A, Bataineh M and Guizani M 2002 Advances in optical switching and networking: past, present, and future *IEEE Southeast Conf. 2002* pp 405–13

[3] Pei S C 1991 Ultrafast multibeatlength all-optical fibre switch *Electron. Lett.* **27** 1209–11

[4] Hedekvist P O, Karlsson M and Andrekson P A 1997 Fiber four-wave mixing demultiplexing with inherent parametric amplification *J. Lightwave Technol.* **15** 2051–8

[5] Chang C L, Yeh C Y, Smith M K, Smith K M, Rosette R A and Straede R 2000 Fiber optic switching apparatus and method *US Patent* 6,044,186

[6] Morey W W and Glomb W L 1991 Incorporated Bragg filter temperature compensated optical waveguide device *US Patent* 5,042,898

[7] Yoffe G W, Krug P A, Ouellette F and Thorncarft D A 1995 Passive temperature -compensating package for optical fiber gratings *Appl. Opt.* **34** 6859–61

[8] Fan K C, Lin W L, Chung T T, Wang H Y and Wu L P 2005 A miniature low-cost and high reliability 1×2 mechanical optical switch *J. Micromech. Microeng.* **15** 1565–70

[9] Dautartas M F, Blonder G E, Wong Y H and Chen Y C 1995 A self-aligned optical subassembly for multi-mode devices *IEEE Trans. Compon. Packag. Manuf. Technol.* B **18** 552–7

[10] Sutherland J, George G, Van der Groen S and Krusius J P 1996 Alignment tolerance measurements and optical coupling modeling for optoelectronic array interface assemblies *Proc. 46th Electronic Components and Technology Conf. (28–31 May)* pp 480–6

[11] Liu A Q, Zhang X M, Murukeshan V M, Zhang Q X, Zou Q B and Uppili S 2002 An optical crossconnect (OXC) using drawbridge micromirrors *Sensors Actuators* A **97–8** 227–38

[12] Nagaoka S 1990 Latching type single-mode fiber switch *Electron. Lett.* **26** 744–5

[13] Lau P G and Buist R J 1997 Calculation of thermoelectric power generation performance using finite element analysis *Proc. 16th Int. Conf. on Thermoelectrics* pp 563–6

[14] Chung T T, Lee C C and Fan K C 2006 Optimum design of a 1×2 mechanical optical switch *Struct. Multidiscip. Optim.* **31** 229–40

[15] Bejan A 1993 *Heat Transfer* (Canada: Wiley)

[16] Fox R W and McDonald A T 1998 *Introduction to Fluid Mechanics* (New York: Wiley)

[17] Fan K C, Lin W L and Wang H Y 2005 The development of automatic light tracing alignment technique for a 1×2 mechanical optical switch *9th Int. Conf. on Mechatronics Technology (5–8 December, Kuala Lumpur, Malaysia)* ICMT-171